

Metal/Slag Separation Behavior of CCA with Various Slag Systems and Effect of Slag Composition on the Content of Sulfur and Phosphorus in Iron Nugget

Ji-Ook PARK and Sung-Mo JUNG*

Graduate Institute of Ferrous Technology (GIFT), Pohang University of Science and Technology (POSTECH), Cheongam-ro 77, Pohang, 790-784 Korea.

(Received on February 27, 2015; accepted on April 14, 2015)

The smelting reduction of high Al_2O_3 ores with petroleum coke containing various slags was investigated in the temperature range of 1 673 to 1 773 K with a special focus on the effect of slag composition on the desulfurization and dephosphorization of iron nugget. The efficient smelting reduction of the carbon composite agglomerate (CCA) would greatly be affected by the mineralogy of iron ore, coal and additives used in the preparation of CCA although the design of final slag composition is important for the ultimate separation of metal and slag. The separation of metal and slag in the reduction progress was retarded due to the delayed melting of CCA with high basicity slag of low SiO_2 content. The content of sulfur in iron nugget decreased to about 0.07 mass% by incorporating high basicity slag to CCA at the temperatures above 1 723 K, which is compatible with the minimum sulfur content in iron of the conventional ITmk3 process (0.05–0.07 mass%). About 80–90% of phosphorus in CCA was eliminated using high basicity slag ($\text{CaO-Al}_2\text{O}_3$) at 1 723 K, which is believed to be much better dephosphorization efficiency compared with the conventional process.

KEY WORDS: carbon composite agglomerate; high Al_2O_3 iron ore; direct smelting reduction; carburization; metal/slag separation; desulfurization; dephosphorization.

1. Introduction

Due to the depletion of high grade lump iron ores in the world, great efforts have been made to utilize low grade iron ores such as ore fines, magnetite ores and high Al_2O_3 ores. In particular, high Al_2O_3 iron ores cause several critical problems in the blast furnace (BF) operation.^{1,2)} The proportion of direct reduced iron (DRI) used in electric arc furnace (EAF) operation has been increasing because high quality and low-residual scrap, which had traditionally been used in EAFs to produce high quality steel, is in shortage.³⁾ The gas-based direct reduction (DR) processes such as MIDREX or HYL III are becoming more and more competitive due to low price of shale gas. Nevertheless, coal-based DRI processes such as rotary kiln or rotary hearth furnace (RHF) are still receiving great attention for producing flat products of steel using virgin iron.⁴⁾ However, extensive understanding of DRI production technology using high Al_2O_3 ores is limited in direct reduction ironmaking processes.

The slag composition in direct smelting reduction process is not so demanding compared with that of BF process. In this respect, the smelting reduction of carbon composite agglomerate (CCA) containing high basicity slag in terms of RHF was proposed to utilize high Al_2O_3 ores in the previous study.⁵⁾ The volume of high basicity slag could be decreased

compared with that of relatively high SiO_2 slag, and high desulfurization capacity could also be achieved. In examining the feasibility of using CCA containing high basicity slag, the effect of $\text{CaO-Al}_2\text{O}_3$ slag of high basicity on the reduction of CCA and separation of metal and slag were previously investigated.^{5,6)}

It is generally understood that the molten slag of high basicity is beneficial for both desulfurization and dephosphorization.⁷⁾ Therefore, high basicity slag can be utilized in the direct smelting reduction of CCA such as ITmk3 or Hi-QIP process to decrease the content of sulfur and phosphorus contained in the final iron nugget product. In order to confirm the feasibility, the reduction experiments of CCA containing high basicity slag were carried out in the temperature range of 1 673 to 1 773 K. Accordingly, the addition of various slag systems to CCA comprised of high Al_2O_3 ores and coke might have significant influence on the separation of metal and slag. Furthermore, by measuring the content of sulfur and phosphorus in the separated iron nugget and slag after the experiments were completed, the effect of slag composition on the desulfurization and dephosphorization of iron nugget was clarified.

2. Experimental

2.1. Materials Preparation

The experiments used the limonitic laterite iron ores con-

* Corresponding author: E-mail: smjung@postech.ac.kr
DOI: <http://dx.doi.org/10.2355/isijinternational.ISIJINT-2015-118>

taining high Al_2O_3 and low SiO_2 and petroleum coke of low ash as reductant. Detailed chemical information is shown in **Tables 1** and **2**, respectively. Both ore and coke were sieved to be in the range of 100–150 μm .

As shown in Table 2, the petroleum coke contains negligible amount of ash while its sulfur content is very high up to 5.7 mass%. To decrease its melting temperature as low as possible by high basicity slag (Slag D in **Fig. 1**), some additives such as CaO and SiO_2 were required. General coke contains ash component and its ash contains quite large amount of SiO_2 . Since SiO_2 content in Slag D of high basicity is very low (about 6 mass%), coke addition of high SiO_2 requires huge amount of CaO (or Al_2O_3) additives to achieve Slag D as a final slag composition after CCA reduction is finished. In this respect, coke of low ash could facilitate the great decrease in the final slag volume. In the conventional slag composition such as Slag A and Slag B in **Fig. 1**, the sulfur content of coal might be a critical problem since S in coal increases that in separated iron, but high desulfurization ability of CaO– Al_2O_3 -based Slag D would

compensate such effect.

2.2. Experimental Procedure

Based on the gangue composition of the high Al_2O_3 ores and the mixing ratio of ore to coke, four different slag systems were designed by adding CaO, Al_2O_3 or SiO_2 to obtain Slag A, Slag B, Slag C and Slag D for the final slag compositions after the reaction was finished as shown in **Fig. 1**. Mixing ratio of each sample is represented in **Table 3**. Melting behavior of each slag predicted by FactSage was shown in **Fig. 2**.⁸⁾ Slag C and Slag D have relatively higher melting temperatures than the others. The molar ratio of carbon to oxygen (C/O) was fixed to be unity in all the CCAs. About 5 g of pressed CCA was placed into a graphite crucible (20 mm ID \times 25 mm OD \times 50 mm height) and reacted in the temperature range of 1 673 to 1 773 K in atmospheric condition. Then the crucible was quickly put into to a muffle furnace for the isothermal reaction and quickly taken out from the furnace after reaction. High purity Ar gas was blown onto the sample to minimize any reaction during cooling. Reaction time was varied from 5 to 20 min. After reaction, the metal and slag were separated and supplied for the chemical analyses of the iron nugget. The carbon and sulfur were analyzed by LECO combustion method, and phosphorus was quantified by inductively coupled plasma-atomic emission spectroscopy (ICP-AES). In addition, the

Table 1. Chemical composition of limonitic laterite ore used in the present study (mass%).

	T.Fe	Fe^{2+}	M.Fe	SiO_2	Al_2O_3	Ni	P	S
Limonitic Laterite	42.52	0.42	–	5.11	7.80	1.5	0.03	1.58

Table 2. Chemical composition of petroleum coke used in the lab scale test.

Proximate analysis (mass%, db)				Ultimate analysis (mass%, daf)				
VM	FC	Ash	IM	C	H	N	S	O ^a
10.97	87.7	0.06	0.68	87.25	3.70	1.03	5.73	2.29

^aBy difference

Table 3. Mixing conditions of the pellets with various slag systems.

	Ore (g)	Petro coke (g)	CaO (g)	SiO_2 (g)	Al_2O_3 (g)
CCA_no Slag	3.0	0.47	–	–	–
CCA_Slag A	3.0	0.47	0.36	0.81	–
CCA_Slag B	3.0	0.47	0.47	0.32	–
CCA_Slag C	3.0	0.47	0.18	0.02	–
CCA_Slag D	3.0	0.47	1.21	–	0.73

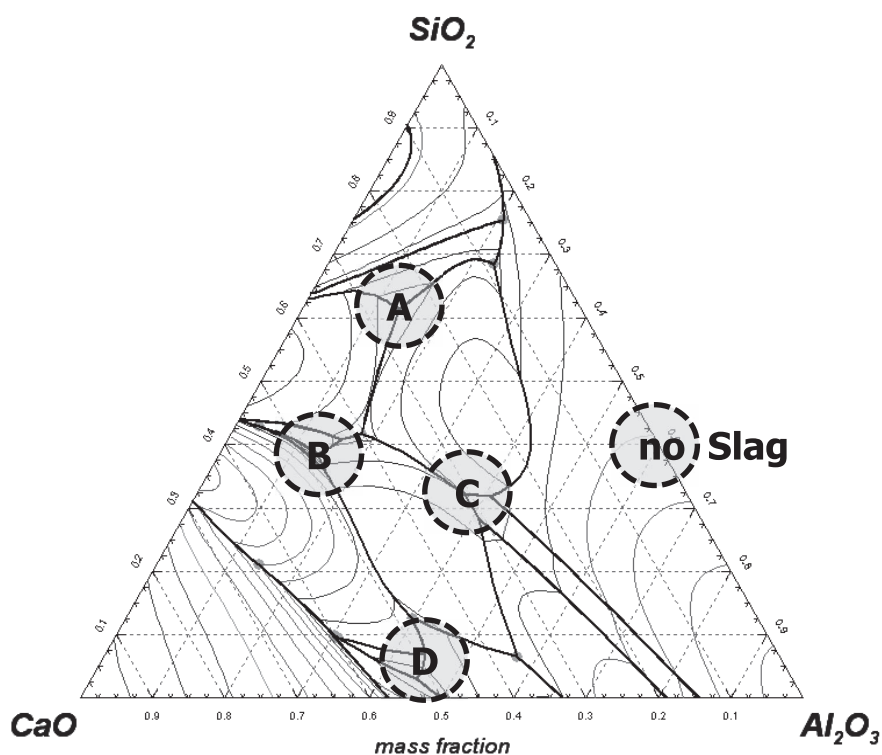


Fig. 1. Compositions of the slags (Slag A, Slag B, Slag C and Slag D) used in the present study.

slag composition was analyzed by X-ray fluorescence spectrometry (XRF).

3. Results and Discussion

3.1. Metal/Slag Separation Behavior of CCA with Various Slag Systems in the Smelting Reduction

Figure 3 shows the reacted samples with various slag systems as a function of temperature. It is clearly indicated that the introduction of low melting slag systems (CCA_Slag A–CCA_Slag D) clearly promoted the separation of metal and slag while CCA_no Slag showed very poor separation behavior even at 1773 K. Among them, CCA_Slag C and CCA_Slag D showed relatively poor separation at 1673 K than the others. As discussed in the previous study,⁶⁾ it is more difficult to develop the direct carburization and melting of solid iron (Fe) in the case of CaO–Al₂O₃-based slag of high melting temperature compared with CaO–SiO₂-based slag. In Fig. 4, it can be known that the carburization degrees of reduced iron (Fe) in CCA_Slag C and CCA_Slag D are relatively low and are not enough to form Fe–C melt at 1673 K. Therefore, the current results show that the slag melting temperatures could be nicely cor-

related with the carburization of iron followed by the separation of metal and slag as discussed in the previous study.⁶⁾ Nevertheless, the separation temperature of CCA comprised of ore and coke is higher than that of Fe–C–slag system.⁶⁾ This is because the slag in Fe–C–slag system does not include FeO that should appear in the reduction progress of CCA containing the slag systems being considered in the present study. As demonstrated in the previous works,^{6,9)} the surface tension of the liquid slag initially formed in CCA would exert attraction force on Fe and carbon in a way that Fe can quickly be carburized in close touch with carbon, which results in the formation of liquid Fe–C melt. Therefore, it is required to extensively compare the melting temperatures, viscosities and surface tensions of CaO–SiO₂- and CaO–Al₂O₃-based slags. As shown in Table 4, since the slag of low viscosity and high surface tension would exert higher attraction force between the particles of Fe and carbon, it might be expected that CaO–Al₂O₃-based slag would play more conclusive role in making Fe and carbon contact each other. However, since CaO–SiO₂-based slags actually showed better separation of metal and slag, it is believed that the initial melting temperatures of Slag A, Slag B and Slag C could further be decreased due to the formation of

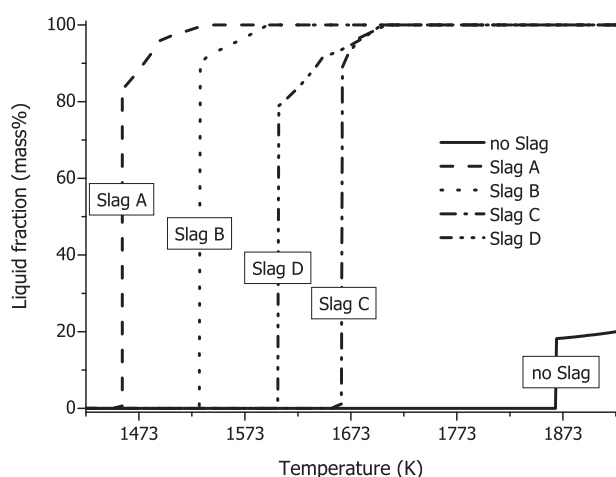


Fig. 2. Melting behavior of slag systems used in the present study.

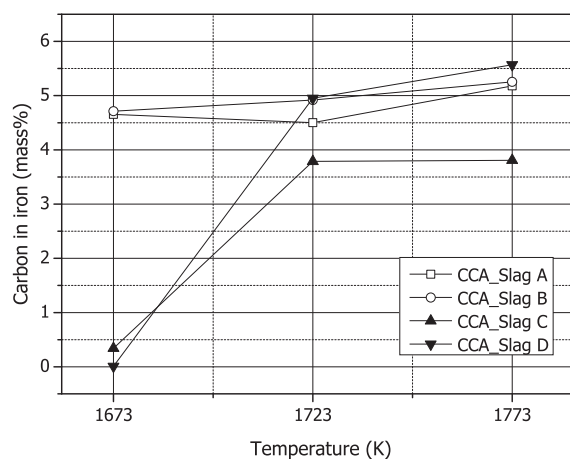


Fig. 4. Effects of temperature and slag composition on the content of carbon in separated iron nuggets.

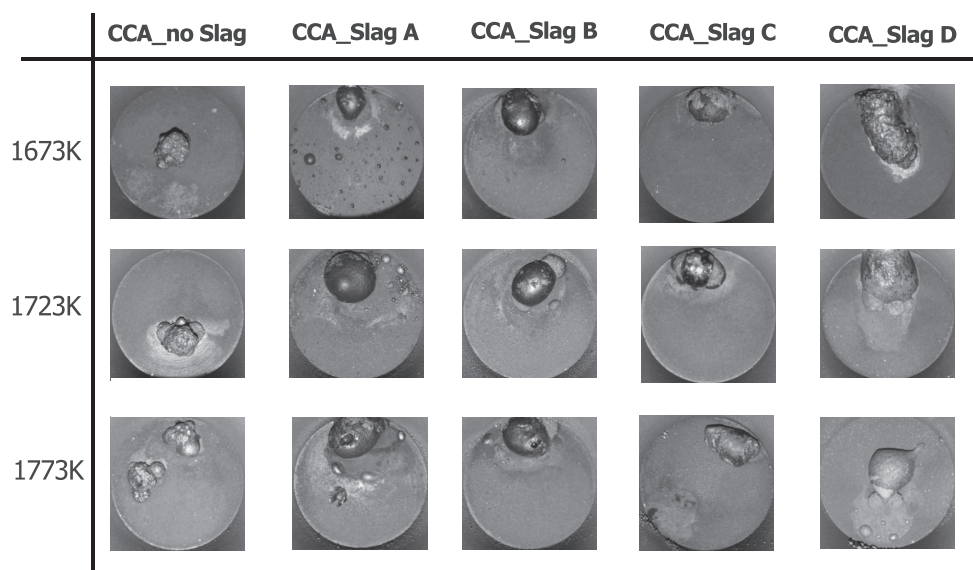


Fig. 3. Sample images of CCA containing various slag systems with changing reaction temperature.

Table 4. Comparison of physical properties of CaO–SiO₂- and CaO–Al₂O₃-based slags.

Properties	CaO–SiO ₂ -based slag	CaO–Al ₂ O ₃ -based slag	References
Melting temp. (°C)	~1 185°C (Slag A)	~1 437°C (Slag D)	8)
	~1 333°C (Slag B)		
	~1 392°C (Slag C)		
Viscosity	High	Low	11)
Surface tension	Low	High	11)
Intermediate phases estimated in reduction progress	2FeO·SiO ₂	CaO·Fe ₂ O ₃	–

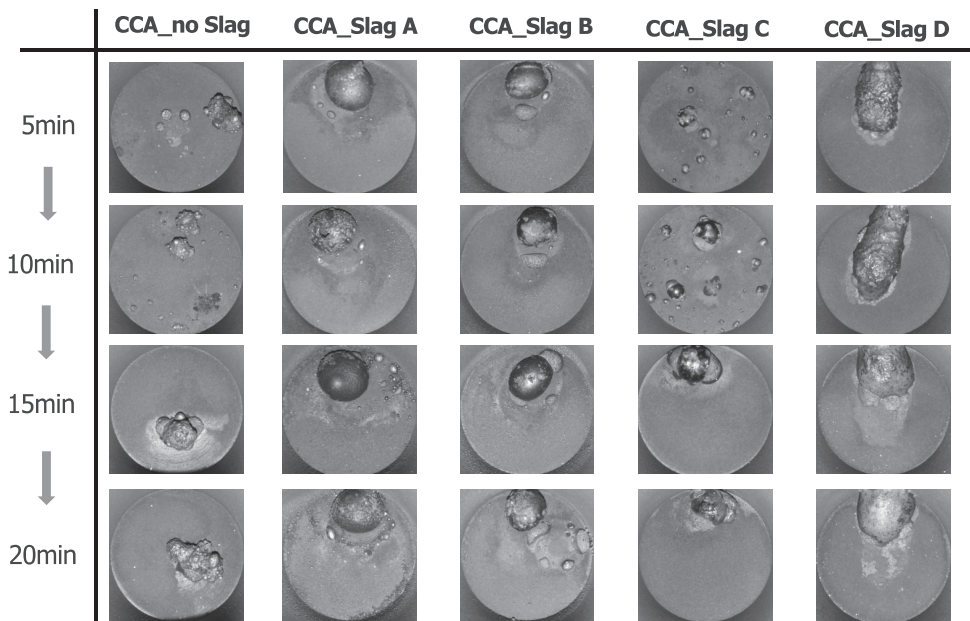


Fig. 5. Images of reacted samples containing various slag systems with time at 1 723 K.

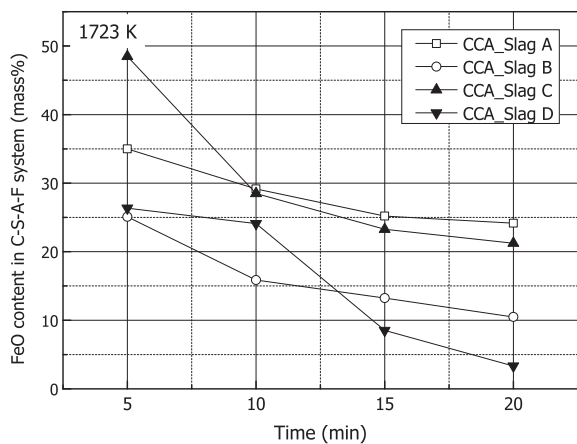


Fig. 6. Change in FeO content of separated slags with reaction time at 1 723 K.

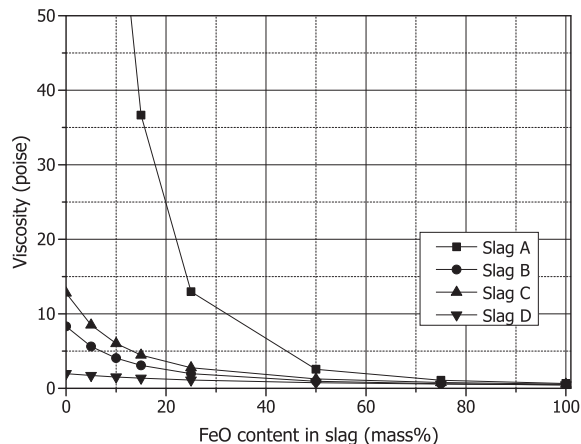


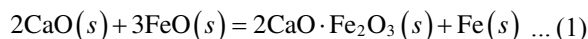
Fig. 7. Effect of FeO content on the viscosities of slag systems at 1 723 K.

intermediate phase, fayalite (2FeO·SiO₂) whose melting point is about 1 210°C.¹⁰⁾ Therefore, it could be considered that the melting temperature of a slag might be the dominating factor affecting the separation of metal and slag in the reduction of CCA compared with other physical properties of the slag, *i.e.* viscosity, surface tension, *etc.*

In order to clarify the effect of FeO produced in the reduction progress of CCA (ore and coke) on the separation of metal and slag, the reaction time was changed from 5 to 20 min. **Figure 5** shows the images of the reacted samples containing various slag systems with reaction time at 1 723

K. CCA_Slag D clearly showed the insufficient melting of slag and poor separation of metal and slag until 10 min. As shown in **Fig. 6**, FeO content continued to decrease with reaction time in all the cases. In general, the melting temperature of slag decreases with increasing FeO content.¹¹⁾ Furthermore, the viscosity predicted by FactSage calculation module⁸⁾ in **Fig. 7** indicates that the decrease in FeO content increases the viscosity in the current slag system, which is in good agreement with the experimental data shown in literature.¹¹⁾ Although taking the positive effects of low melting temperature and low viscosities of slags on the

smooth separation of metal and slag into account, the rapid decrease and low content of FeO might not be the only dominant factor affecting the poor separation of metal and slag in CCA containing high basicity slag. As shown in Fig. 7, due to the formation of fayalite ($2\text{FeO}\cdot\text{SiO}_2$), the decrease in FeO content of Slag A and Slag C has more influence on the increase in their melting temperature, which results in the increase of their viscosities compared with the cases of Slag B and Slag D. In addition, since the activities of CaO in CaO– Al_2O_3 -based slag (Slag D) are higher than those in CaO– SiO_2 -based slags (Slag A, Slag B and Slag C),¹¹⁾ CaO in Slag D would favorably combine with FeO, the intermediate oxide in the reduction progress of iron oxide which would also participate in the reaction to form dicalcium ferrite as follows:¹⁰⁾

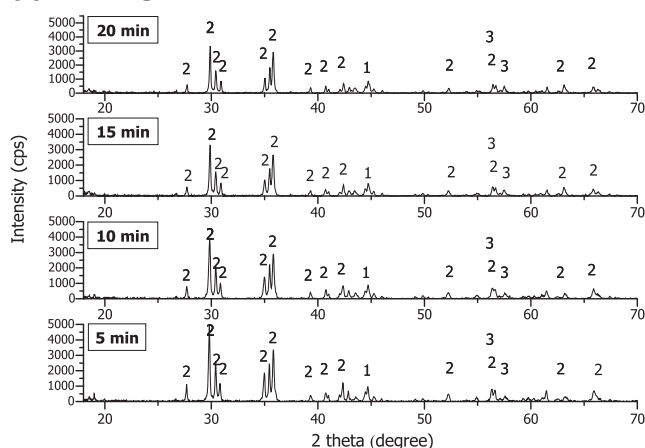


This would rapidly increase the reducibility of the ore in CCA, which affects the reduction of CCA_Slag D in such a way that Slag D retains high melting temperature and high viscosities. Accordingly, Slag D would make less contribution to the carburization of reduced Fe in the reduction of CCA, which results in the poor separation of metal and slag.

Furthermore, it is believed that such poor separation in CCA_Slag D might be ascribed to inhomogeneous melting

of slag resulted from high melting temperature of Slag D. The XRD patterns of the slags separated in the reduction of CCA_Slag A represent no remarkable change in the major peaks with changing reaction time as shown in Fig. 8(a). On the other hand, XRD patterns of the slags separated during the reduction of CCA_Slag D shown in Fig. 8(b) indicated the drastic change in between the major peaks measured at 5/10 min and those at 15/20 min. Unlike the pre-melted slag dealt with in the previous study,⁶⁾ the gangue constituents of the ore are inhomogeneously distributed through CCA. These gangue components should be in close contact to form the final slag of low melting temperature. In the case of CaO– SiO_2 -based slags, the slag of low liquidus temperature evolved from fayalite ($2\text{FeO}\cdot\text{SiO}_2$) might facilitate the further increase in the amount of molten slag due to the high fluidity of initial molten slag. However, in the case of CCA_Slag D containing negligible amount of SiO_2 , it is believed that the homogeneous melting of slag was not sufficiently carried out compared with CCA_Slag A and CCA_Slag B containing higher SiO_2 . Actually, the decrease of SiO_2 content in slag increased the time required for the separation of metal and slag as shown in Fig. 9. This clearly indicates that the efficient smelting reduction of CCA would greatly be affected by the mineralogy of iron ore, coal and additives used in the preparation of CCA although the design of final slag composition is important for the ultimate separation of metal and slag.

(a) CCA_Slag A



(b) CCA_Slag D

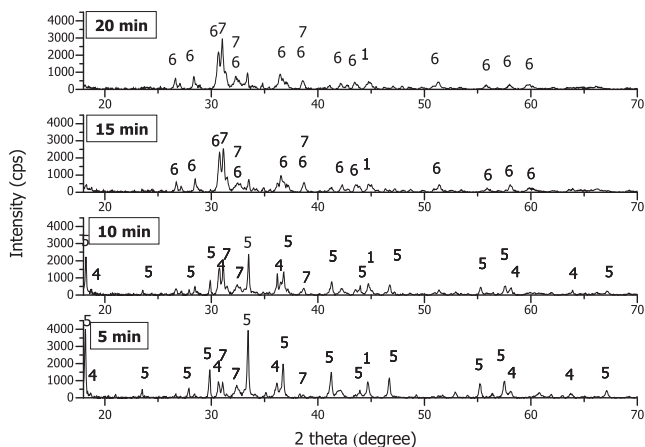


Fig. 8. XRD patterns of the slags separated in the reduction of (a) CCA_Slag A and (b) CCA_Slag D at 1723 K. (1-Fe, 2-Ca(Mg, Fe) Si_2O_6 , 3-MnMg Si_2O_6 , 4-Mg(Fe, Al) O_4 , 5- $\text{Ca}_{12}\text{Al}_{14}\text{O}_{33}$, 6- $\text{Ca}_5\text{Al}_6\text{O}_{14}$ and 7- $\text{Ca}_{20}\text{Al}_{26}\text{Mg}_3\text{Si}_3\text{O}_{68}$).

3.2. Behavior of Sulfur in the Smelting Reduction Process

The effects of temperature and reaction time on the content of sulfur in separated iron is shown in Fig. 10. At the temperatures above 1723 K, the content of sulfur decreased to about 0.07 mass% by incorporating high basicity slag to CCA. The minimum content of sulfur in the iron produced by the conventional ITmk3 process was reported to be 0.05–0.07 mass% when using conventional ore and coal.¹²⁾ For instance, in case CCA comprised of hematite (0.012 mass% S) and coal (0.59 mass% S) was heated to 1573 K for 30 min in N_2 atmosphere to produce DRI, and the produced DRI was desulfurized by 30 vol% H_2/N_2 atmosphere at 1473 K for 0–30 min, metallic iron was found to contain 0.081–0.134 mass% of sulfur.¹³⁾ Considering that more than 100 and 10 times higher sulfur in laterite ore and petroleum

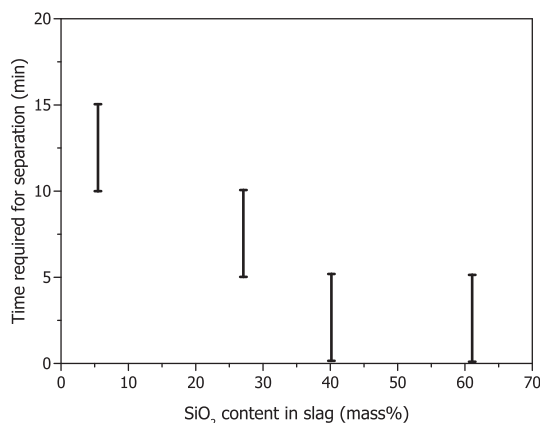


Fig. 9. Effect of SiO_2 content on time required for the separation of metal and slag at 1723 K.

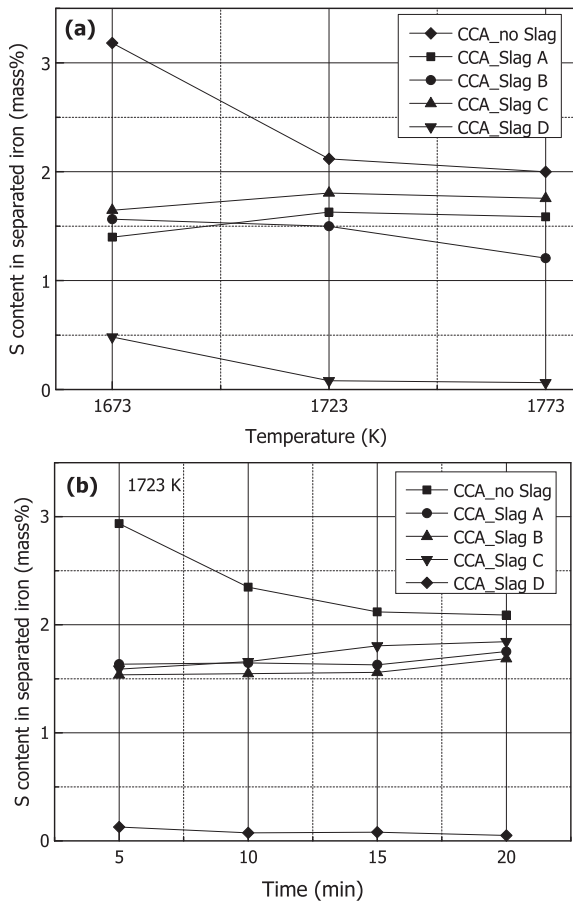
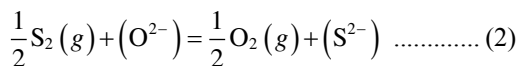


Fig. 10. Effects of (a) temperature and (b) reaction time on sulfur content in separated iron nugget.

coke, respectively, are contained in this study compared with that in the research reported by Inaba and Kimura,¹³⁾ it is very surprising that the lower content of sulfur in iron nugget by about 0.01 mass% was achieved by CCA with high basicity slag in the current study. This is because the activity of CaO in CaO–Al₂O₃-based slag is relatively high.

In the cases of Slag A, Slag B and Slag C, it was found that the changing tendency in the experimental sulfur partition ratio with temperature and reaction time is in good accordance with the calculated sulfide capacity of slags as shown in Fig. 11. The sulfide capacity of slags was calculated by FactSage equilibrium module.⁸⁾ Richardson and Fincham¹⁴⁾ expressed the desulfurization reaction between gas and slag in the oxygen partial pressure lower than 10⁻⁶ atm by Reaction (2), and defined the sulfide capacity, C_{S²⁻} by Eq. (4):



$$K_{(2)} = \frac{a_{S^{2-}} \cdot p_{O_2}^{1/2}}{a_{O^{2-}} \cdot p_{S_2}^{1/2}} = \frac{f_{S^{2-}} \cdot (\text{mass}\%S^{2-}) \cdot p_{O_2}^{1/2}}{a_{O^{2-}} \cdot p_{S_2}^{1/2}} \dots\dots\dots (3)$$

$$C_{S^{2-}} = (\text{mass}\%S^{2-}) \cdot \left(\frac{p_{O_2}}{p_{S_2}}\right)^{1/2} = K_{(2)} \cdot \left(\frac{a_{O^{2-}}}{f_{S^{2-}}}\right) \dots\dots\dots (4)$$

where $a_{S^{2-}}$ and $a_{O^{2-}}$ are the activities of S and O in slag, respectively, and $f_{S^{2-}}$ and (mass%S²⁻) are the activity coefficient and concentration of sulfur in slag, respectively.

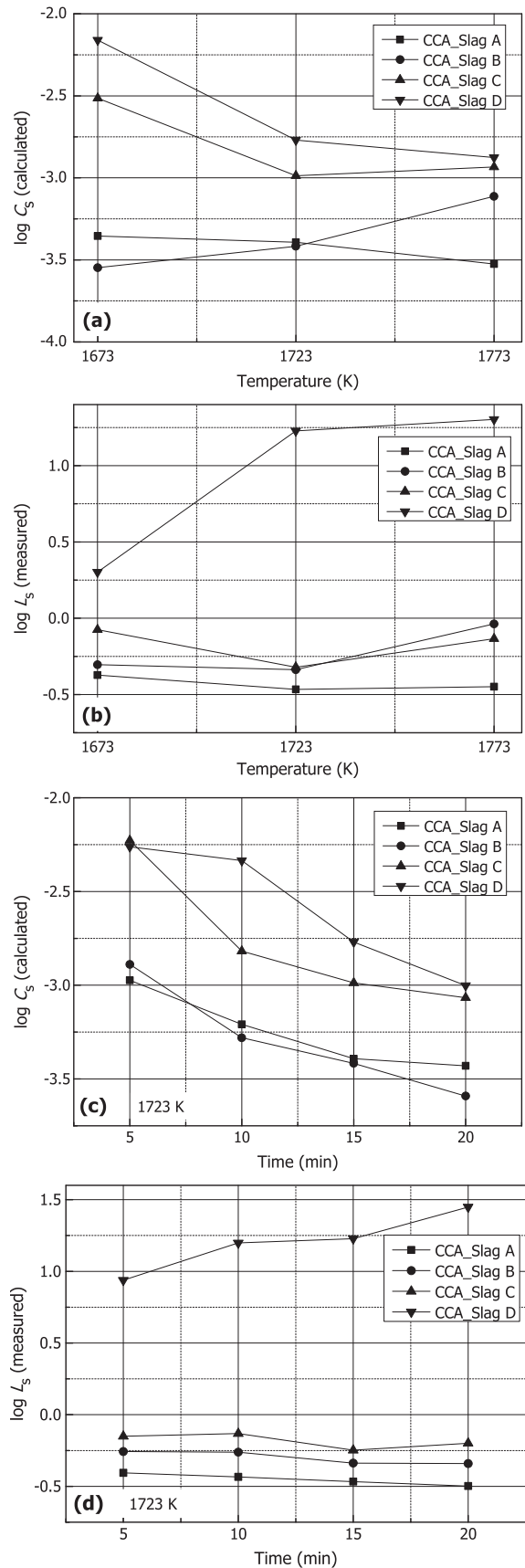
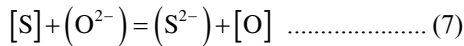
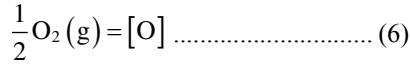
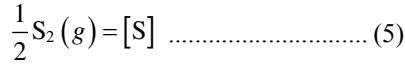


Fig. 11. Effects of temperature and reaction time on calculated and measured values of sulfide capacity and sulfur distribution ratios at 1723 K.

According to Eq. (4), the sulfide capacity increases with raising slag basicity ($a_{O^{2-}}$) and temperature because of the endothermic nature of Eq. (4) with the presence of compo-

nents which have greater affinity for sulfur, such as MnO. The sulfide capacity has been widely used to compare the desulfurizing capacity of metallurgical slags as functions of temperature and slag composition only irrespective of oxygen partial pressure. In addition, the sulfide capacity can be correlated with sulfur distribution ratio between slag and metal by combining Eqs. (2), (5) and (6) as follows:



$$L_s = \frac{(\%S)}{[\%S]} = \frac{f_s \cdot a_{O^{2-}}}{f_{S^{2-}} \cdot a_O} = \frac{f_s}{a_O \cdot K_{(2)}} \cdot C_{S^{2-}} \dots\dots\dots (8)$$

where f_s is the activity coefficient of S in Fe, a_O is the activity of O in Fe, and $K_{(2)}$ is the equilibrium constant of Reaction (2). Although Slag D of high basicity showed some deviation due to the inhomogeneous melting of slag, both estimated sulfide capacity and experimentally measured sulfur partition ratio indicated that the desulfurizing ability of CCA with high basicity slag is still very high.

Another important factor for a slag to be a good desulfurizer is its solubility for sulfide. Since the reciprocal of solubility gives the activity coefficient of sulfide ($f_{S^{2-}}$) as shown in Eq. (4), a larger solubility leads to a larger value for $C_{S^{2-}}$. Besides this effect, the solubility directly affects the amount of slag required for the desired degree of desulfurization. According to Uo *et al.*,¹⁵⁾ the solubility of CaS for the CaO–SiO₂–CaF₂ system showed the maximum values when approaching the composition doubly saturated with CaO and 3CaO–SiO₂. As shown in Fig. 11, the desulfurization degrees in the reduction of CCA_Slag C and CCA_Slag D were greater compared with CCA_Slag A and CCA_Slag B. This is because the activities of CaO in CaO–Al₂O₃-based slag (Slag D) are higher than those in CaO–SiO₂-based slags (Slag A, Slag B and Slag C).¹¹⁾ From this viewpoint, it can be suggested that CCA_Slag D of higher desulfurizing capacity could be used for the smelting reduction of CCA if some additives could be used to decrease the melting temperature of Slag D.

3.3. Behavior of Phosphorus (P) in the Smelting Reduction Process

Effects of temperature and reaction time on the content of phosphorus in separated iron is shown in Fig. 12. Compared with phosphorus content in conventional Itmk3 process (about 0.43 mass%),¹⁶⁾ CCA_Slag B and CCA_Slag D showed relatively lower content of phosphorus where 80–90% of P was decreased by using Slag B and Slag D (high Al₂O₃ slag) at 1723 K. As is similar to the treatment relating the sulfide capacity, based on the dephosphorization reaction between gas and slag by Reaction (9), the phosphate capacity can be calculated by Eq. (11):

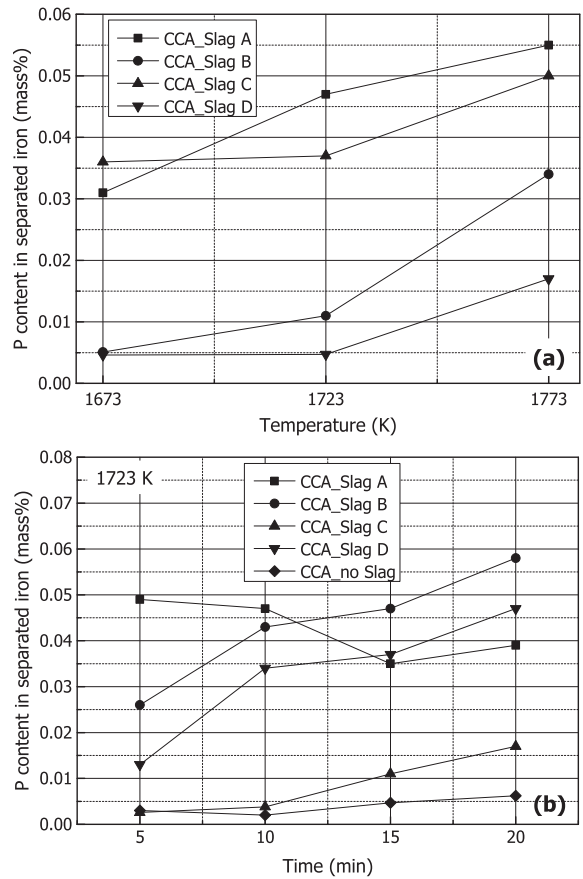
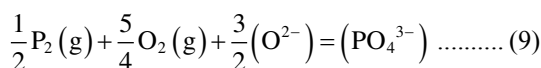
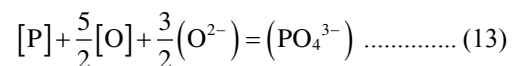


Fig. 12. Effects of temperature and reaction time on the content of phosphorus in separated iron nuggets.

$$K_{(9)} = \frac{a_{PO_4^{3-}}}{a_{O^{2-}}^{3/4} \cdot p_{P_2}^{1/2} \cdot p_{O_2}^{5/4}} = \frac{f_{PO_4^{3-}} \cdot (\text{mass}\%PO_4^{3-})}{a_{O^{2-}}^{3/4} \cdot p_{P_2}^{1/2} \cdot p_{O_2}^{5/4}} \dots (10)$$

$$C_{PO_4^{3-}} = \frac{(\text{mass}\%PO_4^{3-})}{p_{P_2}^{1/2} \cdot p_{O_2}^{5/4}} = K_{(9)} \cdot \left(\frac{a_{O^{2-}}^{3/2}}{f_{PO_4^{3-}}} \right) \dots\dots\dots (11)$$

where $a_{PO_4^{3-}}$ and $a_{O^{2-}}$ are the activities of PO_4^{3-} and O in slag, respectively, and $f_{PO_4^{3-}}$ and $(\text{mass}\%PO_4^{3-})$ are the activity coefficient and concentration of PO_4^{3-} in slag, respectively. $K_{(9)}$ is the equilibrium constant of Reaction (9). In addition, with the help of Eq. (12), the phosphorus reaction between slag and metal can be expressed by Eq. (13), which allows to represent the phosphorus partition ratio by Eq. (14):

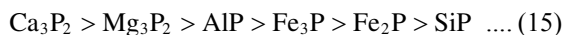


$$L_P = \frac{(\text{mass}\%PO_4^{3-})}{[\text{mass}\%P]} = K_{(13)} \cdot \frac{f_P \cdot a_O^{5/2} \cdot a_{O^{2-}}^{3/2}}{f_{PO_4^{3-}}} \dots\dots (14)$$

where f_P is the activity coefficient of P in Fe, a_O is the activity of O in Fe, and $K_{(13)}$ is the equilibrium constant of Reaction (13).

The calculation of $C_{PO_4^{3-}}$ is similar to that of $C_{S^{2-}}$, but there was some deviation from the behavior of phosphorus

in the current system. Possible explanations on such mismatch between calculated $C_{\text{PO}_4^{3-}}$ and experimental L_P are two folds. Firstly, phosphide can be formed in the progress of reaction. Although the slags contain some amount of FeO, the oxygen potential in gas atmosphere is expected to be much lower than the oxygen partial pressure determined by FeO/Fe equilibrium due to the carbon rich in coke and graphite crucible. In the dephosphorization reaction between slag and metal, phosphide can also be formed when p_{O_2} is low. Critical oxygen potential for the stability of phosphide and phosphate varies with slag composition and temperature, but it is generally much lower than the oxygen potential by FeO/Fe equilibrium. It can be estimated that the oxygen partial pressure lower than 10^{-11} atm is good enough for the formation of Fe above 1673 K.¹⁷⁾ For instance, Momokawa and Sano¹⁸⁾ reported that 10^{-18} atm is the critical value for CaO–Al₂O₃ melt at 1823 K, and Eiji and Moro-Oka¹⁹⁾ similarly estimated $10^{-18.4}$ atm to be the critical oxygen potential for CaO–SiO₂–MnO–CaF₂ slag at 1573 K.¹⁹⁾ In general, it is difficult to expect the existence of phosphide together with FeO in slag. Nevertheless, carbon-saturated melt can exist together with FeO-containing slag in the current condition. Therefore, phosphide can locally exist at the FeO-depleted region of slag in contact with carbon-saturated iron. Once the phosphorus in metal is transferred to slag, phosphide can immediately be changed to phosphate due to high oxygen potential of the slag. From the standard free energies of formation for metal phosphides, the tendency to form phosphides decreases in the order as follows:²⁰⁾



Maramba and Eric²¹⁾ previously reported the improved dephosphorization of Fe alloy by CaO in reducing atmosphere. Since Slag B and Slag D have relatively high amount of CaO than the others, it is reasonable to observe high dephosphorization degrees by Slag B and Slag D as shown in Fig. 12 if phosphide formation is one of the factors governing the behavior of phosphorus in the current system. Nevertheless, since the coexisting FeO in the current system is not truly in equilibrium with carbon-saturated Fe melt, it is not possible to quantitatively explain the formation of phosphide and phosphate at the present stage. In addition, the mismatch between calculated $C_{\text{PO}_4^{3-}}$ and experimental L_P might be ascribed to the vaporization of phosphorus from the metallic Fe. All the cases showed that the sulfur removed in terms of gaseous product corresponds to about 60–70% of total sulfur input. Nevertheless, only 10–20% of phosphorus was lost by gaseous products, which indicates that gaseous phosphorus, *i.e.* P₂ can be dissolved into the iron nugget quickly. The formation of Fe₃P by gaseous phosphorus product was well studied by Sasabe *et al.*²²⁾ and Matinde *et al.*²³⁾ In such a case, the phosphate capacity itself cannot explain the behavior of phosphorus since the reaction between slag and metal is not the only route for the partitioning of phosphorus. The partitioning mechanism of phosphorus between slag and metallic Fe produced in the reduction progress of CCA should further be investigated in future work.

4. Conclusions

The current lab scale tests investigated the direct smelting reduction of CCA containing high basicity slag for the production of iron nugget. From the results, the following conclusions were obtained:

- (1) Iron nugget was successfully produced by direct smelting reduction of CCA comprised of high Al₂O₃ ore and petroleum coke of high S and no ash, which was homogeneously mixed with high basicity slag at 1723 K.
- (2) The smelting reduction of CCA with high basicity slag of low SiO₂ content made slag melting slowed down, which results in the delayed separation of metal and slag. Nevertheless, the sulfur content in iron nugget produced using CCA with high basicity slag was much lower than those by other slag systems at the early stage.
- (3) Due to the high sulfide capacity of high basicity slag, the sulfur content in iron nugget was lower than 0.1 mass%, which is a similar value obtained with conventionally operated method in spite of abnormally high sulfur content in the petroleum coke.
- (4) About 80–90% of phosphorus was removed by using high basicity slag (CaO–Al₂O₃ slag) at 1723 K, which is much better than the dephosphorization by the conventional process.

Acknowledgements

The authors are grateful to POSCO for their valuable comments and financial support.

REFERENCES

- 1) L. Lu, R. J. Holmes and J. R. Manuel: *ISIJ Int.*, **47** (2007), 349.
- 2) A. Cores, A. Babich, M. Muñiz, S. Ferreira and J. Mochon: *ISIJ Int.*, **50** (2010), 1089.
- 3) F. Globler and R. C. A. Minnitt: *J. South African Inst. of Min. Metall.*, **99** (1999), 111.
- 4) S. Inaba: *Tetsu-to-Hagané*, **87** (2001), 221.
- 5) J. O. Park and S.-M. Jung: *Metall. Mater. Trans. B*, (2015), **46B** (2015), 1207.
- 6) J. O. Park, I.-H. Jeong, S.-M. Jung and Y. Sasaki: *ISIJ Int.*, **54** (2014), 1530.
- 7) N. Sano, W.-K. Lu, P. V. Riboud and M. Maeda: *Advanced Physical Chemistry for Process Metallurgy*, Academic Press, San Diego, CA, USA, (1997), 51.
- 8) C. W. Bale, E. Bélisle, P. Chartrand, S. A. Deckerov, G. Eriksson, K. Hack, I.-H. Jung, Y.-B. Kang, J. Melançon, A. D. Pelton, C. Robelin and S. Petersen: *Calphad*, **33** (2009), 295.
- 9) H. S. Kim, J. G. Kim and Y. Sasaki: *ISIJ Int.*, **50** (2010), 1099.
- 10) A. K. Biswas: *Principles of Blast Furnace Ironmaking*, SBA Pub., Calcutta, India, (1981), 108, 227.
- 11) Verein Deutscher Eisenhüttenleute: *Slag Atlas*, 2nd ed., Verlag Stahleisen GmbH, Düsseldorf, (1995), 126, 226, 229, 356, 359, 415, 420.
- 12) H. Michishita and H. Tanaka: *Kobelco Tech. Rev.*, **29** (2010), 69.
- 13) S. Inaba and Y. Kimura: *ISIJ Int.*, **44** (2004), 2112.
- 14) F. D. Richardson and C. J. B. Fincham: *J. Iron Steel Inst.*, **178** (1954), 4.
- 15) M. Uo, E. Sakurai, F. Tsukihashi and N. Sano: *Steel Res.*, **60** (1989), 496.
- 16) K. Ohno: Private communication, (2014).
- 17) D. R. Gaskell: *Introduction to the Thermodynamics of Materials*, 4th ed., Taylor & Francis, New York NY, (2003), 359.
- 18) H. Momokawa and Y. Sano: *J. Electron. Mater.*, **21** (1992), 643.
- 19) I. Eiji and A. Moro-Oka: *Trans. Iron Steel Inst. Jpn.*, **28** (1998), 153.
- 20) Q. C. Horn, R. W. Heckel and C. L. Nassaralla: *Metall. Mater. Trans. B*, **29** (1998), 325.
- 21) B. Maramba and R. H. Eric: *Miner. Eng.*, **21** (2008), 132.
- 22) M. Sasabe, Y. Kiyosawa, M. Otsuka, K. Tanaka and M. Tate: *ISIJ Int.*, **31** (1991), 418.
- 23) E. Matinde, Y. Sasaki and M. Hino: *ISIJ Int.*, **48** (2008), 912.